Project and Manufacturing of an Electric and Modular Unmanned Aircraft

Luís Filipe Fraga Eusébio
luis.eusebio@tecnico.ulisboa.pt

Instituto Superior Técnico, Universidade de Lisboa, Portugal

December 2019

Abstract

Due to the extensive panoply of missions performed currently by unmanned aircraft on behalf of the human being, there is the need of implementing one flying system capable of carry out the largest number of differentiated tasks dynamically. With this in mind, this work describes the very first steps on the development of a modular and fully electric unmanned aerial vehicle, adaptable to every specific assignment in a practical and prompt way. This innovation opens a window of opportunities to technological advances and large profits in the aviation market with the development of a single reconfigurable flight platform capable of fulfilling differentiated missions existing presently, usually performed by different aircraft in their geometry and dimensions. It is therefore necessary to design a light weight aircraft model, with the application of simple and recyclable materials, fully electric propulsion and with the capability of performing a conventional, hover and vertical flight. During this work the several phases of an aeronautical design project will be described and accomplished, starting with the conceptual design and the theoretical definition of the several aerodynamic, structural, stability and performance parameters, and also the selection of the required instrumentation; following the phases of preliminary and detailed design with the purpose of performing a computational validation of the previous theoretical parameters and thus ensuring the aeronavegability of the developed configuration; and finishing with the manufacturing and experimental tests of the aircraft model designed for verification of the previous design phases analyses by theoretical and computational methods.
Keywords: Unmanned Aerial Vehicle, Design and Manufacturing Project, Modularity, 3D Printing, Convencional and Vertical Flight

1. Introduction

Over the past few decades, with their growing popularity, several terminologies have been attributed in an attempt to describe unmanned aircraft, including the designations UAV (Unmanned Aerial Vehicle) and UAS (Unmanned Aerial System) in order to make reference to flying machines capable of operating without the human presence on board, composed by other systems apart of the aircraft itself, such as the remote control stations, the communications links, the launching and recovering systems, among others [1]. Other cognames have been assigned to these aircraft, including the RPV (Remoted Piloted Vehicle), RPA (Remoted Piloted Aircraft) and RPAS (Remoted Piloted Aerial System) in order to demonstrate the presence of man in the chain of control of the whole system [2]. Unmanned aviation is not an invention of today's minds, its conception dates back to the 19^{th} century, alongside with the first steps in manned aviation development through primordial concepts lighter than air [3]. From maritime surveillance to cargo transport, from air patrol to passenger transport, from medical assistance support to sports and scientific footage, from search and rescue to natural disasters monitoring, extensive and diversified is the range of applications of modern aviation [4]. The use of UAVs for the fulfilment of these tasks means less operational limitations than conventional manned aircraft, such as the lack of worry about the health and tiredness of the crew, the ability of taking complex decisions in small time frames without presenting physiological limitations during accelerations or manoeuvres and the lower environmental impact and lower energy consumption, with direct reflection on operating costs [5].

2. Background

2.1. Flexcraft Project

The main goal of this work is to design, build and perform flight and ground tests of an 1-by-15 scale prototype in order to validate the airworthiness of the original Flexcraft aircraft. Product of a consortium of portuguese companies and institutions, including IST (Instituto Superior Técnico). The de-

sign of this original aircraft focuses on the principle of flexibility through the adaption to multiple flight scenarios and conditions, giving it the ability to perform both short and vertical take-off and landing (SVTOL) operatioms and also to change its fuselage module depending on the mission performed (such as aerial taxing, forest surveillance, logistic cargo transportation, civil protection or private usage) [6]. Thus, regarding both configurations in figure 1, besides the scaling factor applied to the external structure of the original Flexcraft, the manufacturing of this RPV model should comply with some main assumptions, such as the implementation of a fully electric propulsive system, the use of simple and recyclable materials, the achievement of a low-cost and light-weight final model with the capability to perform SVTOL operations, to have a modular and changeable fuselage and to be flexible in its assembly and transportation.

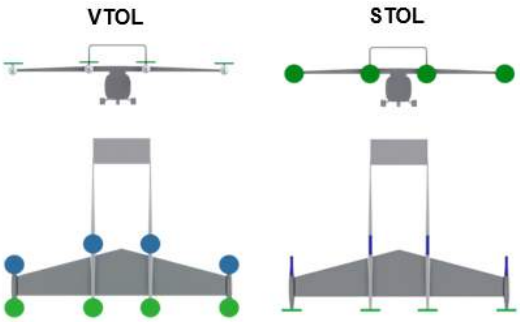

Figure 1: Both STOL a VTOL configurations of the *Flecraft* project [6].

2.2. Aviation Modularity

One kind of reconfigurable aircraft are the hybrid ones, characterized by the ability to realize a double flight envelope, acquiring the advantages of both conventional flight provided by fixed-wing aircraft and also hover flight and VTOL, similar to helicopters. Related with the possibility of switching the type of load module according to the type of mission, modular aircraft have to be adjstable for various purposes in order to maximize their potential of usage [6]. Two possibilities of modularity stand out: a cargo aircraft capable of having its interior quickly remodeled based on the type of mission, with the removal of the passenger seats for the placement of cargo containers; or an aircraft with external pods attached to the outside of the structure.

2.3. Aeronautical Design Process

The design of an aircraft covers four of the main areas of aerospace engineering: aerodynamics, propulsion, control and structures. Each of these areas involves parameters governing the size, shape, weight and performance of the aircraft. At an early stage of the aeronautical design process, the aim is to achieve an optimal combination of all the parameters mentioned, but such perfection is utopian because the improvement of one property can lead to the regression of another. The design process of a new aircraft comprises three distinct phases: conceptual, preliminary and detailed design. During the construction, assembly and operation phases more design and modification phases may arise to correct or improve certain unforeseen details [7].

Starting with the conceptual design where are defined the following main topics: configuration design, structural dimensions, maximum take off weight, instrumentation and performance. It is necessary to determine whether the proposed solution can meet the imposed requirements. This phase corresponds to a cyclical process of changes and improvements around several structural designs, including the analysis and definition of the main characteristics, such as: wing design, weight, fuselage configuration, tail design, implementation of canards, distribution and sizing of the propulsion system, estimation of the fuel or batteries weight, distribution of the internal electronic components and the computation of the weight, aerodynamic and performance parameters [8] [9].

The preliminary design phase aims to increase the credibility and reliability of the previously chosen design by performing detailed computational analyses. A 3D computational model of the complete aircraft and all its integral systems must be performed in order to facilitate the understanding and visualization of the entire layout, positioning of the various electrical and propulsion components, assembly and disassembly mechanisms for maintenance and/or replacement of parts/components and observation of interactions and movements of certain parts of the aircraft. In addition, a FEA (Finite Element Analysis) should be performed to understand the structural response and integrity during flight conditions, as well as CFD (Computational Fluid Dynamics) analysis to redefine the aerodynamic shape of the aircraft. Also, a weight and balance analysis should be performed to achieve model stability [8] [9].

Since this is an input phase for the full scale aircraft development that will lead to its manufacture, in the detailed design it is necessary to perform a thorough description and analysis of each component present in the aircraft, through 3D computational models, geometric designs or manufacturing specifications (including geometric drawings, materials requirements and assembly instructions). Experimental ground and flight tests should be carried out at this stage in order to identify possible anomalies and, consequently, changes to be implemented [8] [9].

3. Conceptual Design

In order to prove the airworthiness of a larger scale aircraft, in the design of this 1-by-15 model there will be no changes in the type of wings, dimensions (scaled), type of tail, number of engines and their locations, airfoils of the several lifting surfaces, position of the landing gears, the aerodynamic and performance parameters, among others. Therefore, there will occur a discussion on: the sizing and type of propulsion used; materials of the several components; fuselage configuration; MTOW; electrical system and estimation of the required energy; estimation of the range and endurance; determination of the cruise and stall speeds; distribution of the instrumentation; type of landing gears; method of assembly and transportation; flight envelope; design point; among others.

3.1. Sizing and Scaling

Regarding the weight of this RPV, no direct scaling factor was applied in order to achieve a greater freedom of the CG (center of gravity) position and, consequently, an adequate SM (static margin) value. A MTOW value between 2 and 3 kg for this UAV was initially predicted.

Regarding the sizing of the external structural components, such dimensions were obtained through the three-dimensional a Computer-Aided Design (CAD) model of the 1-by-10 scaled model of the Flexcraft aircraft, represented in the figure 2. For this purpose, Siemens NX 12.0 software was used, which comprises several computational tools, such as CAD and CAM (Computer-Aided Manufacturing), allowing the development and modeling from individual simple parts to complex assemblies.

Figure 2: 3D CAD model of the 1-by-10 Flexcraft scaled version [10].

The main general dimensions of the 1-by-15 aircraft to be built were obtained by direct scaling of the model 1-by-10 (which were based on the full size aircraft), are as following:

- Maximum width equal to 1 m of length, corresponding to the wingspan in this case;
- Total length of approximately 70 cm;
- Total height of approximately 30 cm.

As for the fuselage, with an aerodynamic Sears-Haack shape, by direct scaling of the dimensions defined for the original aircraft in [6], a length of 0.413 m and a maximum width equivalent to 0.107 m were obtained. This aircraft model has a total of four landing gears, and after applying the scale factor 10/15 to the model of the figure 2. The values of 230.0 mm and 10.8 mm of length and average diameter, respectively, were obtained for the two front landing gears. Similarly, for the rear landing gears were obtained a length of 127.0 mm and an average diameter of 7.5 mm.

Some parameters of the original aircraft related to wing dimensions were obtained, such as the planform area (S), wing tip or root chord (c_{tip} and c_{root}), wingspan (b), dihedral (Γ), aspect ratio (AR), mean aerodynamic chord ($\bar{c}$), taper ratio (λ) and sweep angle (Λ). After the application of the scale factor, in the table 1 can be found the main parameters of the different lifting surfaces, such as the main wing, horizontal stabilizer and vertical stabilizers [6].

Table 1: Scaled dimensions of the lifting devices.

	Main Wing	Horiz. Stab.	Vert. Stab.
S [m^2]	0.159	0.033	0.010
b [m]	1.0	0.267	0.133
AR [-]	6.28	2.16	1.77
Γ [°]	1.0	0	0
Λ [°]	0	0	35.0
c_{root} [m]	0.227	0.124	0.076
c_{tip} [m]	0.091	0.124	0.076
λ [-]	0.4	1.0	1.0

This aircraft configuration exhibits a total of seven control surfaces, including two flaps, two flaperons, two rudders and one elevator. Both flaps and flaperons have a maximum deflection of 35° for take-off and 40° for landing conditions. Both rudders and the elevator have a maximum deflection of 30° for maneuvers.

3.2. Aerodynamics

A previous understanding of the aerodynamic characteristics is crucial to obtain an estimation of the operating limitations and capabilities of this model during its flight envelope. These properties pass through the maximum lift coefficient ($C_{L_{max}}$), maximum aerodynamic resistance coefficient ($C_{D_{max}}$), ratio between the two mentioned coefficients, friction coefficient, among others. The NACA64-A415 airfoil is used in the main wing, the vertical stabilizers are made up of a NACA0012 airfoil and, lastly, the NACA0009 airfoil forms the horizontal stabilizer.

Using the XFLR5© software, it was possible to design a three-dimensional representation of the wing surfaces with the respective dimensions and positions on 1-by-15 model and, successively, to obtain some relevant aerodynamic properties, considering finite and infinite wing analysis. It was con-

sidered a Reynolds number interval between 50000 and 400000 with increments of 25000, a zero Mach value for an inviscid flow simulation, an angle of attack interval between -5° and 15° with increments of 0.5°, and a parameter of turbulence level, N_{crit}, equal to 9, typical value used in the e^N transition prediction method [10].

The referred aerodynamics are established in table 2 with and without the presence of control surfaces, simulating the condition of cruise flight and take-off, respectively. To obtain these results, the RPV model was assigned with a mass of 3 kg as an initial estimation, an angle of attack between -5° and 15° and a variable displacement speed by definition of the XFLR5© software. For the simulations the Vortex Lattice Method (VLM) was used.

Table 2: Aerodynamic coefficients for cruise and take-off conditions.

	Cruise	Take-Off
C_{Lmax}	1.437 (α=15°)	2.235 (α=15°)
C_{Dmax}	0.106 (α=15°)	0.221 (α=15°)
$(C_L/C_D)_{max}$	13.557 (α=15°)	17.118 (α=-5°)
$C_{L\alpha=0°}$	0.212	1.079
$C_{D\alpha=0°}$	0.015	0.065
$(C_L/C_D)_{\alpha=0°}$	86.50	16.707

The results obtained differ from the real values due to the absence of fuselage, landing gears, central booms and lateral motor casings as a recommendation of the software due to modeling complexity.

3.3. Instrumentation

The operation of a RPV model requires the integration of several instruments responsible for different tasks in flight, regarding the propulsion, control, performance, telemetry and structural support.

Starting with the propulsion system, it was necessary to calculate the amount of power required to be implemented in the aircraft. The required power was calculated by two different methodologies in order to obtain different results for comparison and validation. The first methodology involves the equality of the power-to-weight ratio of the original Flexcraft model in the 1-by-15 one. It represents a conservative approach in the sense that the real operating conditions of the original model are replicated for this smaller scaled RPV. Thus, a total power of 710.35 W was obtained, meaning a value of 177.59 W for each motor. The second methodology aims to obtain the theoretical power value required for both cruising and take-off situations through the equation 1 [7]. For the cruise flight condition, the thrust value is obtained by the corresponding aerodynamic resistance, according to the equation 2.

$$P = U \cdot T \tag{1}$$

$$T = D = \frac{1}{2}\rho \cdot S \cdot V_C^2 \cdot C_{Dmax} \tag{2}$$

where was assumed a cruising speed (V_C) of 25 m/s, a MTOW of 3 kg and the aerodynamic coefficients were taken from the table 2. For climb condition was considered an angle of climb equal to 15°, a climb rate of 12.5° and a climb speed equal to 12.08 m/s. Additionally, was considered a propulsive efficiency of 60%. For the cruise flight condition a total power value of 268.83 W was obtained, meaning a power of 67.21 W for each of the four motors. For climb condition was predicted a total value of 460.97 W and an individual value of 115.24 W. Thus, the brushless electric motor **HobbyWing XRotor 2205 2600 Kv Titanium G2 SL BL** was selected, having a maximum power equal to 420 W, a thrust force equivalent to 1.25 kg, an unit weight of 29.5 g. By compatibility of the electric motors chosen, were selected the propellers **Dalprops Cyclons Series 5050 tri-bladed**, with a single weight of 3.9 g. Additionally, was selected the ESC (Electronic Speed Controller) **HobbyWing XRotor 30A Micro 2-4S BL Heli**, with a maximum current of 40 A and continuous current of 30 A. Each one of these ESC weights 7 g.

For this aircraft at scale 1 by 15, a LiPo (Lithium and Polyethylene Oxide) batteries was chosen due to its high storage capacity and energy discharge and to its small size and low weight. The **Tattu LiPo 2300MAH 14.8V 45C 4S1P** battery was then chosen to supply power to the propulsive system of this RPV model. It has an unity weight of 230.5 g. In order to estimate the endurance of this aircraft, the equation 3 was used:

$$t = \frac{C \cdot 0.001 \cdot T_d \cdot V}{MTOW \cdot P_{1kg}} \tag{3}$$

where C and V represent the battery capacity and voltage, respectively. T_d, equal to 80%, regards the maximum percentage of discharge allowed for LiPo batteries to prevent damages. And P_{1kg} is related to the amount of power required to sustain 1 kg of the aircraft fully equipped. Thus, were estimated the endurance times of 10.13 min. and 3.54 min. for both operating conditions of cruise and climb flight, respectively.

For the servo's implementation, were used two methodologies, a computational one through PredimRC© tool and a theoretical one using the equation 4:

$$\tau = 8.5 \times 10^{-6} \left[\bar{c}^2 \cdot V^2 \cdot L \frac{sen(S1) \cdot tan(S1)}{tan(S2)} \right] \tag{4}$$

where $S1$ and $S2$ represent the maximum deflection angles of the control surface and of the servo, respectively. Of all the control surfaces, a maximum torque value of 0.34 kg.cm was obtained. Planning the choice of the servos with an increased margin, was selected the **Turnigy TG9e Eco Micro**

Servo 1.5kg for this UAV. It has a reduced weight of 9 g and dimensions of 23 × 12.2 × 29 mm that allow an easier integration in the aircraft.

Regarding the electronic and avionic instruments that this 1-by-15 model aims at testing before their integration in the 1-by-10 model, follows a list with their main characteristics:

- **Pixhawk Cube 2.1** with a weight of 39 g, dimensions 94.5 × 44 × 31 mm and a unit cost of 260 euros;
- GPS antenna **Here+ V2 RTK GNSS** with a weight of 49 g, a diameter of 60 mm and a height equal to 17 mm;
- Telemetry transmitter and receiver **Holybro Telemetry RadioSet V2 500mW 433MHz** with a weight of 110 g, dimensions 26×53×10.7 mm and a unit cost of 46.74 euros;
- Radio control ***Receiver RC X8R*** having a weight of 16.8 g, dimensions 46.5 × 27 × 14 mm and a unit price of 29.58 euros;
- **Digital Differential Airspeed Sensor Kit** with a weight equal to 14 g and a price of 49.90 euros each.

The front landing gears chosen to support this 1-by-15 model have a total height of 205 mm and a unit weight of 35 g and an external diameter of 10 mm. Each one can withstand a weight equal to 9 kg. The rear landing gears have an adjustable height with a wheel of 25 mm and a unit weight of 14.2 g.

3.4. Performance

In the figure 3 it is possible to observe the assigned mission profile for both the STOL and VTOL settings of this UAV.

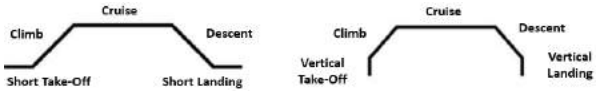

Figure 3: Mission profiles for STOL and VTOL conditions.

As for the runway distance required to perform the short take-off, by scaling the 1000 ft assigned to the original aircraft, an estimated distance of 20.33 m was considered. As referred previously, it was estimated a cruise velocity of 25 m/s, corresponding to a stall speed of 11.63 m/s and 14.50 m/s with and without high-lift devices, respectively. Also, a climb/take-off speed of 13.95 m/s was estimated. The endurance values previously estimated correspond to 10.13 min. and 3.54 min. for cruise and climb, respectively.

A flight envelope for the different flight conditions was defined, considering the interaction of wind gusts with the application of the airworthiness requirements and safety factors. Thus, it was possible to analyze the capabilities and limitations of the aircraft's structure depending on the speed and load factor given during the V-n diagram. It was considered the limits of 4.4 and -1.8 for the load factor of this RPV as a "General - Utility Aviation" [11]. For the flight envelope, presented in the figure 4, was computed a maximum cruise speed (V_F) of 32.5 m/s, a dive speed (V_D) of 35.0 m/s and a maximum and minimum maneuver speed (V_A and V_H) of 21.41 m/s and 14.97 m/s, respectively. Two wind gusts were considered with normal gusts velocities, $\hat{u}$, 15 m/s and 7.5 m/s for level flight and dive, respectively, which cause increases in the load factor [11].

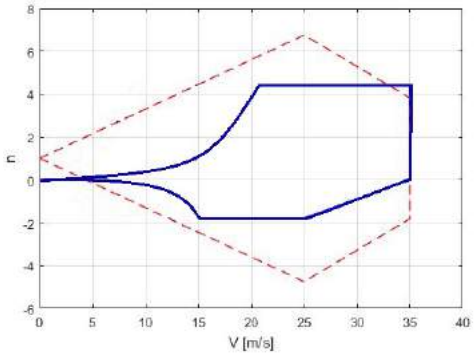

Figure 4: Flight and gusts envelope obtained.

4. Preliminary and Detailed Design

In this chapter, a three-dimensional CAD model of the entire structure of this RPV was created, with the respective placement of the components and assignment of the materials, allowing the performance of a structural analysis of the critical components and an analysis of static and dynamic stability.

4.1. Materials Analysis and Selection

The XPS (Extruded Polystyrene) foam was chosen for all the lifting and control surfaces of this RPV model due to its relatively low price, its simplicity of handling and surface treatment and, above all, its low density that allows for a reduced weight without compromising its resistance to structural forces of impact and compression.

For the 3D printed components, the use of PLA (Polylactic Acid) was chosen instead of ABS (Acrylonitrile Butadiene Styrene), due to its feasible printing properties without releasing toxic vapours, its lower extrusion temperature and an acceptable bending, compression and elongation rigidity for this application scenario.

For structural reinforcement of the wings of this aircraft bidirectional carbon fiber strips were implemented. When compared to glass fiber, the carbon fiber, despite being less economical, presents a higher modulus of elasticity and a lower density.

Finally, as a solution for structural strengthening of the main wings, stainless steel beams were introduced. As for the control surfaces, in order to not affect the position of the CG, it was opted for the use of carbon rods of reduced thickness. Table 3 shows the values of density (ρ), in kg/m^3, modulus of elasticity (E), in GPa, and yield stress (σ_{ced}), in MPa, of the referred materials.

Table 3: Mechanical properties of the materials used.

	XPS	PLA	Carbon Fiber	Stainless Steel	Carbon Rod
ρ	34.296	1240	1310	7850	1760
E	0.017	1.190	42	210	230
σ	0.361	20.07	14.352	500	3530

4.2. CAD Modelling and Structural Improvements

The software Siemens NX 12.0© was used to model the several components of this aircraft, namely the side and central fairings, the canopy and its cover, the booms that link the rear empennage, the lifting surfaces, the control surfaces, the corners connecting the vertical and horizontal stabilizers, the instrumentation, the structural reinforcements, the fuselage, among others. Most of the PLA components referred were designed with several parts, allowing an easy detachment for an access to the interior of them for replacement or maintenance of instrumentation or cabling.

The most advantageous configuration for the manufacturing of this model was decided to be a combination of XPS foam for the wings and PLA plastic for the other structural parts whose geometries are too complex to be produced manually with XPS foam. This configuration despite representing a higher production cost and structural weight it allows the internal transportation of the avionics with an increased structural stiffness and with a minimal disruption of external flow.

Due to structural unforeseen events that arose during the computational analysis, several changes were implemented. In order to obtain an acceptable SM for a stabled and controlled flight, several lead ballast masses were placed in the front fairings and in the canopy in order to move the CG forwards. Two stainless steel bars were used for structural reinforcement and movement of the CG (center of gravity) position inside of the main wings near the leading edge. Supports for the avionics and battery inside the canopy were design in order to prevent them from moving during the flight and to define their pre-established location to achieve the outlined balance. Additionally, different PLA plastic fittings were modeled to allow for an easier removal and replacement of the servos without damaging the wing surfaces. In the figure 5 is possible to visualize the complete STOL configuration.

Figure 5: STOL configuration of this RPV model.

4.3. Stability Analysis

Once the geometric modelling of the aircraft was completed with the placement of the several components in their final locations and with the respective materials assigned, a theoretical MTOW value equal to 2965.7 g was obtained for the STOL configuration with fuselage, close to the 3 kg initially planned. Additionally, a CG was calculated with the following coordinates: $x_{CG} = 61.3$ mm, $y_{CG} = -0.1$ mm and $z_{CG} = 2.7$ mm. The asymmetry observed along y resulted from the weight's differences of the telemetry devices inside the canopy.

The same procedure was taken for the STOL configuration without the fuselage, and also through a computational methodology with Simens NX 12.0 for validation and comparison of the results obtained. In the case that the fuselage is connected to the aircraft, a difference of 2.5mm was obtained for the x_{CG} between methodologies, meaning a deviation equivalent to 4.3%. The differences in values obtained for the position of the CG in the longitudinal axis are justified by the absence of certain components in the analyses carried out computationally, including the landing gears, GPS antenna, the pitot tube, screws, cabling and the carbon fibers.

Through the equation 5 were obtained the values of SM, assuming a neutral point (NP) value of 74.3 mm, obtained from semi-empirical expressions. Both theoretically and computationally, with or without fuselage, SM values between 5.73% and 7.76% were obtained, showing positive stable values and within the expected limits for control (between 5% and 25%).

$$K_n = \frac{x_{NP} - x_{CG}}{MAC} \tag{5}$$

Then, the first moments of inertia of the RPV model were computed with the Siemens NX 12.0©, with and without fuselage. Thus, the longitudinal and lateral static stability derivatives were estimated through the software XFLR5©. The obtained results confirmed a static stability of this RPV model for both longitudinal and lateral conditions. Complementarily, using the XFLR5© and the characteristics of designed aircraft, out a dynamic stability analysis was carried for longitudinal and lateral conditions. Longitudinally, both short period and phugoid modes are stable. Laterally,

apart from the spiral mode with a reduced positive real value, both roll and Dutch roll modes were stable.

4.4. Structural Analysis

Through the computational tool Nastran of Siemens NX 12.0© with the FEA method, structural analyses of some components were performed to ensure the integrity of the aircraft for the critical loads identified in its flight envelope. The results shall be obtained by applying boundary conditions simulating the static and dynamic environment to which the aircraft is subjected, where the results of maximum deflections, maximum stresses and vibration modes can be analyzed.

Due to the geometric complexity of the components subjected to this structural analysis, it was decided to use quadratic tetrahedral elements CTETRA(10). These elements present a Lagrangean formulation with a total of 10 nodes, i.e., 30 degrees of freedom per element. In order to verify the computational results obtained, Euler-Bernoulli's theoretical methodology was applied for a distributed load along a cantilever beam and for the application of a punctual load at the beam end. Both theoretical conditions aim to simulate the application of an aerodynamic load and the effect of the presence of components in the main wing tips.

From the structural analysis carried out to the main wing using the two methodologies, the need for including stainless steel beams was deemed necessary to support the loads 4.4g and -1.8g of the flight envelope, as well as a force of 5 N at the tip of the wing. A convergence analysis was performed for the mesh of the several components, before running the final simulations. In the figure 6 is possible to observe the structural analysis performed on the main wing reinforced with the steel rod, obtaining a maximum displacement value equal to 20.03 mm and a maximum stress of 120.54 MPa for the application of the maximum load factor (4.4g).

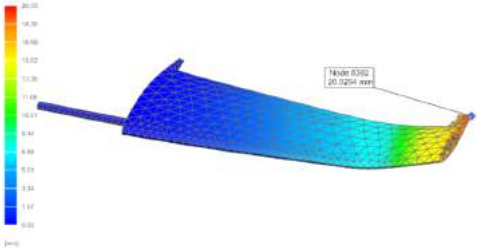

Figure 6: Main wing maximum deflection for a load factor of 4.4g applied.

Additionally, structural analyses were performed to other components of the aircraft in order to determine their responses to the acceleration of the electric motors and to the load applied by the weight of instruments or other adjacent components. There was no maximum deflection value of concern as well as a maximum stress higher than the yield stress value of the material, concluding that the aircraft can withstand the structural loads defined previously.

To complete this phase of structural analysis, the following frequencies of the natural vibration modes were obtained for the main wing, in Hz: 28.6, 118.0, 159.4, 195.8, 285.4 and 404.4.

5. VTOL Configuration

Moving on to the description of the reconfiguration process of this UAV, where the implementation of the capability to perform VTOL flight was obtained by replacing the lateral and frontal structural fairings. A tilting rotors system was implemented as a method for transition between vertical and horizontal flight, representing a simple change and construction mechanism without the need for carrying large structural weights.

In order to calculate the power required for this aircraft to perform hover flight, the actuator disc theory of Rankine was applied (equation 6)[12]:

$$P = k\frac{T^{3/2}}{\sqrt{2\rho A}} \tag{6}$$

where the thrust (T) must equal the total weight of the aircraft (W): $T = W$. Assuming a total mass of 3.5 kg for this VTOL configuration, we obtain a necessary global propulsive force equivalent to 34.34 N. Applying a security factor of 1.3 due to the propulsive system imperfections that may occur, was obtain a value of 44.64 for the needed thrust. With a total of eight electric motors, a propulsive force for each engine of 5.58N was obtained. The variable A corresponds to the total area of actuator disk, equal to 0.1995 m^2. And the empirical correlation factor k, equal to 1.15, called the induced power factor, aims to account for the non-ideal physical effects such as wingtip losses and the approach to a disc when indeed there is a finite number of blades. Therefore were obtained the values of total and individual power (per engine): 330.94 W and 61.32 W, respectively.

About the endurance, it was concluded the need of a second battery to achieve higher flight times. The placement of this second battery was conditioned by the limited space available inside the canopy, the only viable solution was to introduce it inside the fuselage, implying that this VTOL configuration cannot fly without it. This gives an endurance value of approximately 1 min. for an hover flight condition.

The structural reconfiguration consists of replacing the side fairings to introduce the tilting front rotors system (represented in the figure 5) and some parts of the central fairings to add the rear motors to produce only vertical thrust. Due to the removal of the former's front fairings, some new lead ballast

masses inside of the modular fuselage were implemented.

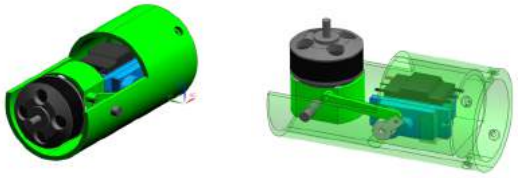

(a) STOL mode. (b) VTOL mode.

Figure 7: Front motor fairings of the VTOL configuration.

For this VTOL configuration, illustrated in the figure 8, a MTOW of 3358.8 g was obtained. As was done for the STOL configuration, the coordinates of the CG were calculated theoretically and computationally. For the VTOL version with the presence of a fuselage, the values of $x_{CG} = 63.8$ mm, $y_{CG} = -0.1$ mm and $z_{CG} = -4.6$ mm were obtained. Between the two methodologies, a deviation of 1.9% for the value of x_{CG} was obtained, with the presence of a coupled fuselage.

Figure 8: VTOL configuration of this RPV model.

After obtaining the respectives moments of inertia of the VTOL configuration, negative static margin values were obtained for the version without fuselage, indicating the mandatory use of it. For that condition, values of 5.25% and 5.84% were obtained by theoretical and computational means, respectively. Also, for both static and dynamic stability variables for this configuration were computed stable values, apart from the spiral mode as it happened in the STOL configuration.

The structures considered critical for the previous version of this aircraft were maintained, but an increase in the structural weight with main concern at the main wing tips was observed. Thus, structural analyses were performed in order to verify the response of the main reinforced wings to the application of a point load of 10 N. These analyses verify the need for implementing of the stainless steel rod as well as its efficiency in the overall stiffness of the wing, proving the structural stiffness of the main wings for both versions (STOL and VTOL) through a conservative load value.

6. Manufacturing Process

Starting with the manufacture of the wing surfaces made of XPS foam, they were obtained through a cutting process machined with a nickel wire at a temperature high enough to pass through the material. This technique involves the use of the JediCut© program which, with the definition of the wing profile and its respective dimensions, allows the design of a finite wing according to the movement of a hot wire in 4 axes. This is a fast, accurate and cheap wing manufacturing technique. The finishing of the wings underwent a subsequent sanding process with a light granulation (320), reducing the roughness of their surfaces. Drilling was then carried out for the passage of wiring, the steel rod and for the fittings of the plastic parts. To increase the structural stiffness, the main wings were subjected to the application of carbon fiber. In order to stimulate the adhesion of both epoxy and carbon fiber to the wings, they were submitted to a vacuum curing process at 80°C for 8 hours. Subsequently, the control surfaces were cut as an hinge operation achieved with the use of double-sided adhesive tape. Finally, the several wings of this aircraft and their moving parts were coated with an OraStick vinyl, apply with heat.

As for the structural components in PLA, they were manufactured through additive manufacturing, better known as 3D printing. For this purpose, a BeeVeryCreative HelloBeePrusa DIY printer was used. After the CAD modeling of each component, a stereolithography (.stl) file was exported, which was introduced in the software Slic3r 1.42.0, allowing for the definition of the printing properties and the extrusion method. Next, a computer numerical command (CNC) format file, called .gcode, was obtained, giving the printing information to the printer through the Pronterface software. For the 3D printed structural components of this model, it was chosen an infill equivalent to 40%, an extrusion temperature equal to 200°C and a layer thickness of 0.3 mm. After the printing, all the PLA parts were subjected to a surface smoothing process through sanding with medium grain (220) and application of two epoxy layers.

Besides the implementation of the stainless steel rods on the main wings and the carbon rods on the control surfaces, were implemented more corrections in this manufactured model. In order to counteract the existing negative dihedral of the main wings, both stainless steel rods were fixed to the central canopy. Also, a galvanized steel wire system was implemented to correct the negative dihedral and the undesired inclination of the side fairings unaccounted for in the CAD model.

After the introduction of the several electrical components, avionics instruments and their cabling, the final configuration of this RPV model was achieved as illustrated in the figures 9 and 10.

Figure 9: STOL final configuration.

Figure 10: VTOL final configuration.

7. Experimental Tests

After the manufacture of the 1-by-15 model of the Flexcraft aircraft, experimental tests were performed on ground in order to inspect in advance the desired conditions for flight performance. The tests include the balance of the propellers, the calibration and analysis of the electric motors, the measurement of the total structural weight and of the CG position and, finally, the measurement of the inertial properties of the fully equipped aircraft for validation and comparison with the values obtained theoretically and computationally.

In the static tests of the electric motors, for a maximum continuous current equal to 25 A, the real values of the maximum electrical and mechanical power were 352.9 W and 196.2 W, respectively, for a 23.58 A of applied current, instead of the ideal value of 420 W. Also, a maximum torque value equivalent to 0.095 N.m was obtained. The idealized value of 1.25 kgf, predicted by the manufacturer of these electric motors, corresponds in fact to a maximum actual value of 0.769 kgf with the selected set of propellers. As for the maximum efficiency observed during the experimental tests, a value of 59.3% was taken for an applied current of 8.0 A.

Using a scale with an accuracy equivalent to 0.001 kg, the values of 2.815 kg and 2.906 kg were obtained for the STOL configuration with and without fuselage, respectively. When compared with the values obtained theoretically, they show a deviation of 2.23% and 2.15%, respectively, in each configuration. To analyze the static equilibrium of this RPV model, four sensors placed on each wheel were used to calculate the difference of weight loads along the model for the CG position determination. For the STOL configuration without fuselage, a total distributed force equivalent to 30,429 N was measured, giving a CG value equal of 62.3 mm from the leading edge, corresponding to a percentual discrepances of 0.75% and 3.41% when compared with the values obtained theoretically and computationally, respectively. Laterally, the aircraft presents a deviation equivalent to 4.5 mm for the left side, value much higher than theoretically predicted.

With the use of a suspended structure (represented in the figure 11) for a free pendulum movement of the aircraft, it was possible to calculate the moments of inertia of the RPV by measuring the periods of oscillation around the axes of rotation. For both measurements of rolling motion (around the x axis) and pitching motion (around the y axis), values of $I_x = 0.1947$ kg.m^3 and $I_y = 0.0671$ kg.m^3 were obtained, respectively. To measure the moment of inertia around the vertical axis a bifilar pendulum was used, resulting in a moment of inertia of $I_z = 0.2179$ kg.m^3 for the movement of yaw. The values of inertia moments obtained exhibit a deviation of 4.35%, 9.44% and 12.31% for the movements of yaw, pitch and roll, respectively, when compared with the values obtained computationally.

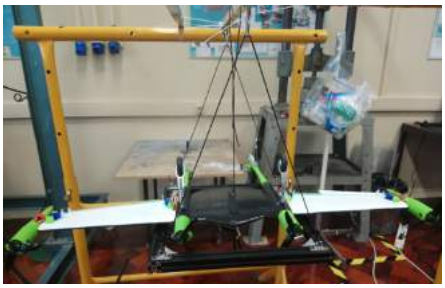

Figure 11: Measuring arrangement.

The percentage deviations observed for the several calculated moments of inertia may be associated with human errors imposed by the measurement of oscillation times in a manual way. In addition, the structure was not made perfect, presenting friction, damping and vibrations, no matter how small they are, inducing errors in the results obtained.

8. Conclusions

Throughout this work the several objectives initially proposed have been accomplished, both at a theoretical and practical level. Starting with a theoretical context of the unmanned aviation development, passing through the description of the Flexcraft project. Additionally, the different phases of an aeronautical design project were completed. In a conceptual design phase, the several requirements and specifications for the development and manufacturing of this RPV were defined, the various scaled dimensions were obtained, the values of the aerodynamic characteristics of the set of wings for the cruise and climb flight conditions were computed and, also, a selection of the instrumentation

was performed in order to accomplish a proper performance during the defined flight envelope.

Following the design process, in the preliminary and detailed phases analyses of the mechanical properties of the different materials present in this aircraft were performed. In addition, a CAD model of all the components of this RPV was design with the inclusion of the multiple instruments in their definitive positions, enabling the performance of computational analyses for stability and structural behavior. The results obtained validated the theoretical outputs and allowed a compliance check of requirements for a successful flight.

In addition, the structural transformations of the STOL configuration in order to obtain the VTOL version, capable of performing hover and vertical flight were explained. The same theoretical and computational analyses were performed to this new configuration as the previous version, proving that this structural change does not induced any harmful results to the expected behavior in flight.

The last chapters served to outline the procedures performed during the manufacturing of this UAV using low-cost materials and simple manufacturing techniques, as well as the description of the different experimental tests carried out in order to confirm the results obtained by theoretical and computational means in the previous phases. The results of the experimental tests confirmed the suitability of this aircraft to perform an effective flight, in terms of propulsion, structural weight and static stability.

In order to alert to what should have been done differently for better final results, a possible change in the dimensions of the central structure of the aircraft is highlighted in order to allow allocating a larger number of components (wiring and the second battery of the VTOL configuration, for example) and increase the accessibility for maintenance and replacement of the instruments. Additionally, in order to achieve a more rigid and compact aircraft, an internal metallic or composite skeleton should have been included, avoiding the need to implement mechanisms to correct unforeseen structural deformations. To increase the validation of the theoretical results obtained, it would be advantageous to carry out experimental aerodynamic tests in the wind tunnel, as well as vibration tests to prove the natural vibration modes frequencies calculated. The limiting time factor prevented the development of computational models with a higher level of detail in aerodynamic and structural analysis than those performed in XFLR5© and Siemens NX 12.0©, respectively.

References

[1] Ignacio Serrano. *Unmanned Aircraft System (UAS) vs. Manned Aircraft System (MAS): A Military Aircraft Study*, 2015. 430.

[2] Suraj G. Gupta, Mangesh M. Chonge, and Dr. P. M. Jawandhiya. *Review of Unmanned Aircraft System (UAS).* International Journal of Advanced Research in Computer Engineering and Technology (IJARCET), Volume 2, Issue 4, april 2013.

[3] Laurence R. Newcome. *Unmanned Aviation: A Brief History of Unmanned Aerial Vehicles.* American Institute of Aeronautics and Astronautics, 2004. ISBN 1563476444.

[4] A. R. Jha. *Theory, Design, and Applications of Unmanned Aerial Vehicles.* CRC Press Taylor and Francis Group, 6000 Broken Sound Parkway NW, Suite 300 Boca Raton, FL 33487-2742, 2016. ISBN 13: 978-1-4987-1542-3.

[5] Nathan Richards Fields. *Advantages and challenges of unmanned aerial vehicle autonomy in the Postheroic age.* Masters Thesis - James Madison University. 205.

[6] R. Reis, M. Quintiães, M. Rodrigues, P. Albuquerque, L. Fartaria, F. Lau, F. Afonso, and J. Vale. *Especificações Técnicas - Especificação de Missão, Utilizadores e Mercado; Especificações da Cpnfiguração do Conceito de Produto; Perfis de Missão, Personas e Mercado; Configuração do Conceito de Produto.* Flexcraft, 2017-09-10. PROJECTO Nº 17805. (In portuguese).

[7] Thomas C. Corke. *Design of Aircraft.* University of Notre Dame, Pearson Education Inc., 2003. ISBN: 0-13-089234-3.

[8] Reg Austin. *Unmanned Aircraft Systems - UAVs Design, Development and Deployment.* A John Wiley and Sons, Ltd., Publication, 2010. ISBN: 978-0-470-05819-0.

[9] Lloyd R. Jenkinson and James F. Marchman. *Aircraft Design Projects for engeneering students.* Butterworth-Heinemann of Elsevier Science, 2003. ISBN: 0-7506-5772-3.

[10] F. Afonso, H. Policarpo, F. Lau, and A. Suleman. *Desenvolvimento - Projeto de VRP.* Flexcraft, 2018-09-21. PROJECTO Nº 17805. (In portuguese).

[11] A. Suleman. *Design Point - Aircraft Design.* Course notes - Instituto Superior Técnico, 2018.

[12] G. J. Leishman. *Principles of Helicopter Aerodynamics.* Cambridge University Press, 2006.